

PERIODICO di MINERALOGIA
established in 1930

*An International Journal of
MINERALOGY, CRYSTALLOGRAPHY, GEOCHEMISTRY,
ORE DEPOSITS, PETROLOGY, VOLCANOLOGY
and applied topics on Environment, Archeometry and Cultural Heritage*

Evidence of basaltic magma intrusions in a trachytic magma chamber at Pantelleria (Italy)

Nunzia Romengo^{1,†}, Patrizia Landi^{2,*} and Silvio Giuseppe Rotolo^{1,3}

¹Università di Palermo, Dipartimento di Scienze della Terra e del Mare, Via Archirafi 36, 90123 Palermo, Italy

²Istituto Nazionale di Geofisica e Vulcanologia, Sezione di Pisa, Via della Faggiola 32, 56126 Pisa, Italy

³Istituto Nazionale di Geofisica e Vulcanologia, Sezione di Palermo, Via U. La Malfa 153, 90146 Palermo, Italy

*Corresponding author: landi@pi.ingv.it

Abstract

In the last 50 ka basalts have erupted outside the margin of the young caldera on the island of Pantelleria. The inner portion of the caldera has instead been filled by trachyte lavas, pantellerite lavas and pumice fall deposits. This paper focuses on a low-volume benmoreite lava topping the trachyte lava pile in the middle of the young caldera.

The mineral chemistry, including trace elements in clinopyroxene (LA-ICP-MS), suggests that benmoreite is a hybrid product resulting from mixing between a trachytic magma and a basaltic end member even more primitive than those erupted during the past 50 ka. The principal inference is that basaltic magmas intruded the trachytic magma chamber below the caldera and were erupted in recent times within the caldera and not only beyond, as the distribution of basaltic centers would suggest. Data are used to discuss the relationship between felsic and mafic magmas at Pantelleria.

Key words: Pantelleria; magma mixing; bimodal magmatism; trachyte; alkali basalt.

Introduction

Pantelleria, the type locality of pantellerites (Fe-rich peralkaline rhyolites), is a small island (13 x 8 km) located in the Sicily Channel Rift Zone between the coasts of Sicily and Tunisia. The Sicily Channel is an NW-SE directed continental rift consisting of three narrow pull-apart basins: the Pantelleria, Linosa and Malta troughs (Finetti et al., 1984; Calanchi et al.,

1989; Catalano et al., 2008). Several submarine and subaerial volcanoes occur in the Sicily Channel (Rotolo et al., 2006 and references therein), including the islands of Pantelleria and Linosa.

The oldest rocks cropping out in Pantelleria are found in the area of Salto La Vecchia-Scauri, near the SW margin of the island; they date to around 320 ka. The SE part of the island is occupied by the 6-km-wide Cinque Denti (or

Monastero) caldera, which formed during the eruption of the Green Tuff around 50 ka ago. It is nested within an older caldera named “La Vecchia caldera” dated 114 ka B.P. (Mahood and Hildreth, 1986; Civetta et al., 1984) or 130-160 ka (Speranza et al., 2011). After the Green Tuff eruption and the related collapse of the Cinque Denti caldera, resurgence started with the eruption of the Monte Gibele-Montagna Grande trachytic lava pile, which filled two thirds of the Cinque Denti Caldera (K/Ar ages: 44-28 ka B.P., Mahood and Hildreth, 1986). A subsequent uplift separated the Montagna Grande block from the Monte Gibele source vent (Mahood and Hildreth, 1986), leading to the formation of the highest peak on the island (Montagna Grande, 836 m asl). Volcanism persisted in the 18-6 ka period, although the frequency of eruptions decreased progressively (Scaillet et al., 2011); it gave rise to a multitude of pantellerite pumice cones, lava flows and lava domes mainly inside the caldera and especially along the trapdoor faults linked to the uplift of Montagna Grande (Mahood and Hildreth, 1986; Civetta et al., 1984; 1988; 1998; Orsi et al., 1991; Rotolo et al., 2007; Speranza et al., 2010; Scaillet et al., 2011).

Peralkaline rhyolitic magmas (pantellerites) are by far the most abundant rock type on the island. Trachytic magmas (mildly peralkaline or slightly metaluminous) are instead limited to intracaldera resurgence (Montagna Grande trachytes) and to the last erupted flow unit of the Green Tuff compound ignimbrite. The other flow units are pantelleritic in composition (Mahood and Hildreth, 1986; Romengo, 2011). Mafic products are very subordinate and occur only outside the caldera rim. The most recent mafic events (about 20,000 years ago; Mahood and Hildreth, 1986) emplaced the Cuddie Rosse and Cuddia Bruciata scoria cones and the related lava flows in the NW part of the island.

From a petrological viewpoint, magmas erupted at Pantelleria are characterized by the mafic-felsic bimodal association common to

several peralkaline centers (the “Daly gap”). Intermediate products between alkali basalts and trachytes-pantellerites were first found as enclaves in trachytes by Villari (1974) and then by Civetta et al. (1984) and Ferla and Meli (2006). Avanzinelli et al. (2004) first described a benmoreite lava probably corresponding to the one studied in this paper, although there is some uncertainty due to the lack of sampling site coordinates. Ferla and Meli (2006) and Avanzinelli et al. (2004) interpreted the benmoreite bulk composition as that of a hybrid rock.

The petrogenesis of pantellerites is highly debated and their origin remains unclear in some aspects, although recent experimental petrology studies (Scaillet and MacDonald, 2001; 2003; 2006; Di Carlo et al., 2010) and petrological investigations (White et al., 2005; 2009) shed light on several aspects of phase equilibria and on the assessment of the pre-eruptive conditions (T , P , fO_2 , H_2O_{melt}). Trachytes are the least evolved felsic rocks on Pantelleria; their study can consequently provide important information on relationships between mafic and felsic magmas. There is a general consensus that pantellerites originate from trachytes via low-pressure crystal fractionation, whereas two contrasting models have been proposed for the origin of the trachytes: (i) protracted fractional crystallization from an alkali basalt parental magma (Civetta et al., 1998; White et al., 2009), or (ii) low-degree remelting of mafic cumulates (Lowenstern and Mahood, 1991; Avanzinelli et al., 2004). The second hypothesis, i.e. no direct consanguinity between mafic and felsic magmas, can perhaps better explain the origin of the Daly gap. Some alternative models are instead consistent with the hypothesis that basalts are parental to trachytes. These models envision: (i) the presence of a zoned magma chamber (trachytic-pantelleritic magmas) that behaves as a density filter for high-viscosity and crystal-rich intermediate magmas (Mungall and Martin,

1995; Peccerillo et al., 2003); (ii) a non-linear increase in silica and crystallinity with decreasing temperature that results in negatively buoyant intermediate magmas (Mushkin et al., 2002; White et al., 2009).

This paper provides petrographic and mineralogical data on a small-volume lava flow of benmoreitic bulk composition that tops the Montagna Grande trachytic lava pile. The mineral chemistry highlights the hybrid origin of this magma, the product of mixing between basaltic and trachytic magmas. The discovery of a mafic magma well inside the caldera, even if as a ghost end-member originating a hybrid rock, has several possible implications for magma evolution and compositional bimodality at

Pantelleria, as well as for magma chamber dynamics.

Sampling and analytical techniques

The benmoreite lava sample (# PAN 0749) was collected at an elevation of 740 m asl (lat 36°46'35", long 11°59'44") from a short (ca 80 m long, 40 m wide), flat lava flow near the top of the Montagna Grande trachytic lava pile (Figure 1). Considering a maximum thickness of four metres, the volume of the lava flow is of the order of 10^4 m³. At the hand-specimen scale the benmoreite rock is dark grey with alkali feldspar phenocrysts (1-2 mm long) > clinopyroxene and equant olivine (up to 4 mm long).

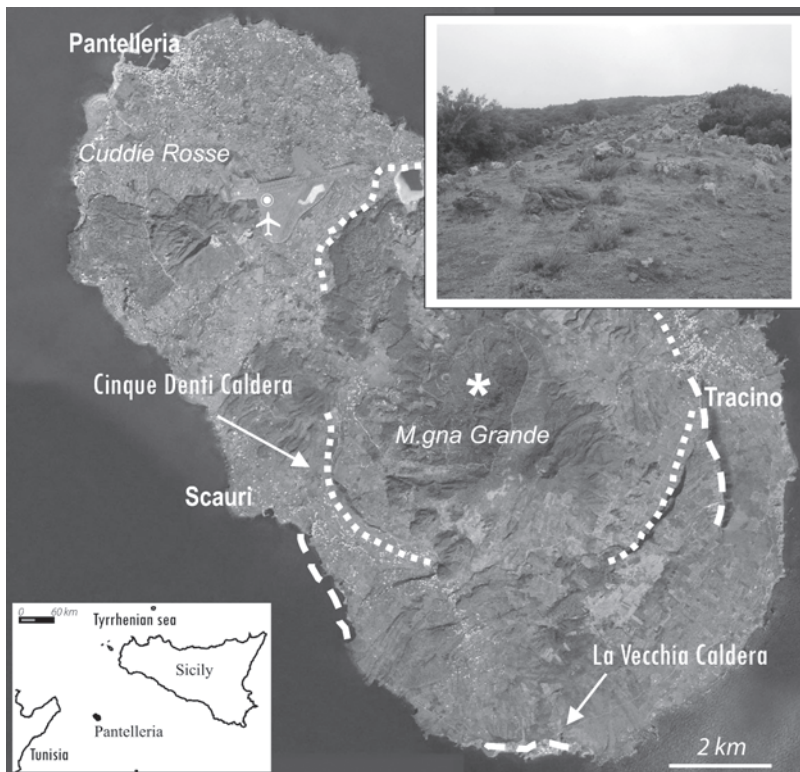


Figure 1. Map of the Island of Pantelleria with the location (star) of the sampled benmoreite lava flow. The upper inset shows a view of the lava outcrop.

Whole-rock major and trace elements were determined using ICP-AES and ICP-MS respectively, at Activation Laboratories Ltd (Ontario, Canada) in accordance with the 4LITHORES protocol. The texture and major element composition of minerals and glassy matrices were determined using a Philips XL30 scanning electron microprobe equipped with EDAX DX4 at the Dipartimento di Scienze della Terra, Pisa University, an OXFORD LEO 440 SEM-EDS housed at Dipartimento di Scienze della Terra e del Mare, Palermo University, (analytical error: 1% for concentrations higher than 15 wt.%, 2% for 5-15 wt.%, 5% for 1-5 wt.%, and 30% for < 1 wt.%) and a JEOL-JXA-8200 electron microprobe (WD/ED combined microanalyzer) at Istituto Nazionale di Geofisica e Vulcanologia in Rome, using 15 kV voltage, a 5 μm beam spot and 5 nA beam current. The WDS analytical error is < 1-3% for major elements. Trace elements in clinopyroxene were obtained by laser ablation-inductively coupled plasma-mass spectrometry (LA-ICP-MS) using a laser source and spectrometer at the Consiglio Nazionale delle Ricerche-Istituto de Geoscienze e Georisorse, Pavia, Italy. The diameter of the sampled area was between 20 and 30 μm . Accuracy is estimated to be better than 5% relative (for further details see Tiepolo et al., 2003).

Mineral chemistry

The lava sample has a benmoreitic composition ($\text{SiO}_2 = 56.6$ wt.% and $\text{Na}_2\text{O} + \text{K}_2\text{O} = 8.4$ wt.%) (Table 1; Figure 2a) with major and trace element contents intermediate between those of the two groups of rocks commonly found at Pantelleria (mafic rocks: alkali-basalts to hawaiites; felsic rocks: trachytes to pantellerites) (Figure 2). It has a highly porphyritic (phenocrysts = 35-45 vol.%) seriate texture. The phenocrysts, in order of decreasing abundance, are: alkali feldspar, plagioclase,

olivine, clinopyroxene and subordinate magnetite and ilmenite. They are all set in a microcrystalline groundmass composed of plagioclase, clinopyroxene and olivine, plus apatite and pyrrhotite as accessory minerals; interstitial glass occurs in minor quantities.

The main feature of this rock is the occurrence of zoned phenocrysts, with both reverse and normal zoning and frequent resorbed cores. Each mineral phase occurs as several texturally and compositionally different typologies.

Feldspars are mainly represented by mm-sized spongy cellular-textured crystals with resorbed areas of anorthoclase $\sim \text{Ab}_{68-70}\text{An}_{6-8}\text{Or}_{23-26}$. The inner portions of crystals show coarsely spongy cellular textures with large cells filled by groundmass material. Finely spongy cellular-textured anorthoclase/oligoclase $\text{Ab}_{68}\text{An}_{19-22}\text{Or}_{10-13}$ occurs either around the anorthoclase-rich near-core areas or as large mantles. Lastly, thin rims of oligoclase $\text{Ab}_{64-65}\text{An}_{27-28}\text{Or}_{7-8}$ encircle phenocrysts and mantle the large cells (Figure 3a). Phenocrysts with resorbed cores of plagioclase $\text{Ab}_{53-63}\text{An}_{32-43}\text{Or}_{3-5}$ surrounded by a finely spongy cellular-textured mantle of oligoclase ($\text{Ab}_{66-67}\text{An}_{23-25}\text{Or}_{9-11}$) are less abundant (Figure 3b). The groundmass is crowded with microphenocrysts (100-200 μm) and microlites (< 50 μm) of plagioclase showing normal zoning (Figure 3c) from $\text{Ab}_{34}\text{An}_{64}\text{Or}_2$ to $\text{Ab}_{66}\text{An}_{25}\text{Or}_9$, all rimmed by anorthoclase ($\text{Ab}_{68}\text{An}_{19}\text{Or}_{14}$). According to Streck (2008 and references therein), spongy cellular textures are attributed to pervasive crystal dissolution in response to disequilibrium events. Mixing between magmas of contrasting composition and temperature may have determined crystal dissolution. Finely spongy cellular-textured anorthoclase/oligoclase were likely produced by re-equilibration between crystals and intermediate melts during and after dissolution of anorthoclase and andesinic plagioclase.

The majority of pyroxene is represented by

augite ($Wo_{40-41}Fs_{25-28}$, $TiO_2 < 0.7$ wt.% and $Al_2O_3 < 0.8$ wt.%, $Mg\# (Mg/Mg+Fe) = 0.52-0.62$) with rounded to lobate shapes and diopsidic rims $< 10 \mu m$ crowded with magnetite and melt inclusions (Figure 4a). Euhedral crystals (up to 1 mm) with diopsidic composition Wo_{43-46}, Fs_{10-15} ($Mg\# 0.75-0.81$) and medium-high TiO_2 (1.4-2.7 wt.%) and Al_2O_3 (3.1-6.0 wt.%) contents are sporadic. Spongy cellular textures and resorption channels near the rim reveal incipient dissolution (Figure 4b). Some other pyroxenes display resorbed augitic cores and up to 150 μm -thick pinkish diopsidic mantles ($Wo_{48}Fs_{12}$) characterized by TiO_2 (2-3

wt.%) and Al_2O_3 (~ 6-7 wt.%) contents that are on the whole higher than those of diopsidic phenocrysts (Figure 4c, d). The groundmass is crowded by skeletal microphenocrysts of pinkish diopsidic/augitic pyroxene (Wo_{40-47}, Fs_{10-14}) with variable TiO_2 (1.4-4 wt.%) and Al_2O_3 (2.8-8.5 wt.%) contents. Sector and normal zoning are common (Figure 4e, f).

Olivine shows a bimodal compositional distribution. The majority of olivine phenocrysts (0.5-1 mm in size) are characterized by normal zoning with large resorbed Fo_{84-86} cores and up to 100 μm -thick Fo_{59-60} rims (Figure 5a). Inclusions of Cr-spinel $Cr/(Cr + Al) = 0.40-0.42$

Table 1. Chemical analyses of the benmoreite lava sample and representative major and trace element contents of clinopyroxene phenocrysts. Representative composition of the pyroxene from C. Rosse trachybasalt is reported for comparison.

Sample	Bulk Rock-PANO749	Clinopyroxene								C. Rosse PAN2-int
		a. ph	a. ph	a. ph	pink	pink	d. ph	d. ph	d. ph	
		px8-int	px15-int	px1-int	px2-rim	px8-rim	px18-core	px18-int	px18-rim	
SiO ₂ wt.%	56.56	51.89	50.88	51.04	46.79	47.28	50.03	47.28	48.61	50.39
TiO ₂	1.94	0.72	0.42	0.54	2.61	2.32	1.37	2.71	1.67	1.29
Al ₂ O ₃	14.78	1.40	0.57	0.63	6.29	6.05	3.27	6.04	5.24	3.54
FeO	8.05	13.49	15.38	17.29	7.73	8.09	8.79	7.73	6.00	8.33
MnO	0.20	0.84	0.96	1.05	0.12	0.15	0.32	0.13	0.10	0.20
MgO	3.25	12.38	11.43	10.36	14.13	13.77	14.60	13.78	14.82	14.69
CaO	5.31	19.41	19.21	18.98	21.02	21.28	20.84	21.61	21.82	21.18
Na ₂ O	5.33	0.65	0.61	0.68	0.45	0.51	0.48	0.43	0.42	0.39
K ₂ O	3.08	-	-	-	-	-	-	-	-	-
P ₂ O ₅	0.60	-	-	-	-	-	-	-	-	-
Cr ₂ O ₃	-	0.00	0.00	0.00	0.24	0.09	0.04	0.02	0.54	0.00
LOI	0.08	-	-	-	-	-	-	-	-	-
Tot	99.19	100.78	99.45	100.55	99.37	99.54	99.73	99.72	99.21	100.01
Wo mol%	-	40.6	40.6	40.2	44.9	45.4	43.2	46.0	46.2	43.9
En	-	36.0	33.6	30.5	42.0	40.9	42.1	40.9	43.7	42.3
Fs	-	23.4	25.8	29.3	13.1	13.7	14.7	13.1	10.1	13.8
Mg#	-	0.62	0.57	0.52	0.77	0.75	0.75	0.76	0.81	0.76

a. ph: augite phenocrysts; d. ph: diopside phenocrysts; pink: pinkish pyroxene. int: interior of the crystal.

Table 1. Continued ...

Sample	Bulk Rock- PANO749	Clinopyroxene									C. Rosse PAN2-int
		a. ph	a. ph	a. ph	pink	pink	d. ph	d. ph	d. ph		
		px8-int	px15-int	px1-int	px2-rim	px8-rim	px18-core	px18-int	px18-rim		
Sc ppm	16	115	128	152	107	99	111	98	100	122	
V	120	101	63	45	257	305	294	337	259	330	
Cr	70	<dl	10	<dl	2111	762	270	884	3676	800	
Co	18	18.46	17.75	16.22	38.96	36.05	35.73	33.14	32.52	40.09	
Ni	50	4.73	2.24	1.96	199.29	162.76	36.16	63.32	202.87	78.06	
Zn	160	212.80	205.74	265.66	40.79	55.79	50.13	26.18	29.01	30.69	
Rb	41	<dl	<dl	<dl	<dl	<dl	<dl	<dl	<dl	<dl	
Sr	352	24.44	21.43	20.18	54.61	63.13	41.20	55.64	65.37	42.35	
Y	45.9	95.73	116.52	114.23	20.69	35.26	15.21	10.79	13.50	14.15	
Zr	405	94.58	108.18	100.09	84.60	125.50	28.59	32.70	56.02	22.79	
Nb	84.9	0.898	0.569	0.478	0.826	1.100	0.322	0.204	0.412	0.142	
Cs	2.1	<dl	<dl	<dl	<dl	<dl	<dl	<dl	<dl	<dl	
Ba	910	0.85	0.10	<dl	<dl	0.05	<dl	0.03	0.10	<dl	
La	61.8	20.87	28.53	28.45	4.78	8.87	2.67	2.36	3.81	1.90	
Ce	123	71.26	92.25	96.68	17.56	31.20	11.32	10.08	14.31	7.73	
Pr	14	12.44	16.23	16.99	3.23	5.65	2.14	1.89	2.52	1.52	
Nd	53.9	68.26	86.04	88.04	17.15	31.60	11.64	10.91	14.25	9.94	
Sm	10.7	18.89	24.18	25.84	6.00	8.80	3.57	3.06	4.53	3.40	
Eu	3.96	4.30	4.59	5.04	1.84	3.02	1.65	1.45	1.50	1.17	
Gd	10.1	21.0	26.6	26.5	5.6	9.5	4.0	3.6	4.2	3.7	
Tb	1.6	3.22	3.99	4.11	0.89	1.41	0.59	0.47	0.58	0.51	
Dy	8.87	21.17	27.19	26.45	5.40	8.20	3.61	2.78	3.68	3.40	
Ho	1.59	3.96	5.29	4.89	0.89	1.54	0.67	0.55	0.55	0.56	
Er	4.54	10.43	13.45	12.57	2.14	4.16	1.65	1.30	1.33	1.49	
Tm	0.644	1.448	1.583	1.753	0.220	0.440	0.162	0.101	0.125	0.173	
Yb	3.96	9.91	11.22	12.08	1.61	2.66	1.07	0.92	0.99	0.99	
Lu	0.579	1.390	2.072	2.040	0.177	0.436	0.148	0.132	0.128	0.145	
Hf	9.4	3.45	4.67	3.59	3.69	5.88	1.38	1.67	2.64	0.96	
Ta	6.01	0.072	0.055	0.019	0.145	0.228	0.032	0.027	0.106	0.032	
Th	8.59	0.042	0.101	0.033	0.056	0.132	0.009	0.009	0.041	<dl	
U	1.88	0.006	0.031	0.012	0.009	<dl	0.005	<dl	0.008	<dl	

a. ph: augite phenocrysts; d. ph: diopside phenocrysts; pink: pinkish pyroxene. int: interior of the crystal.

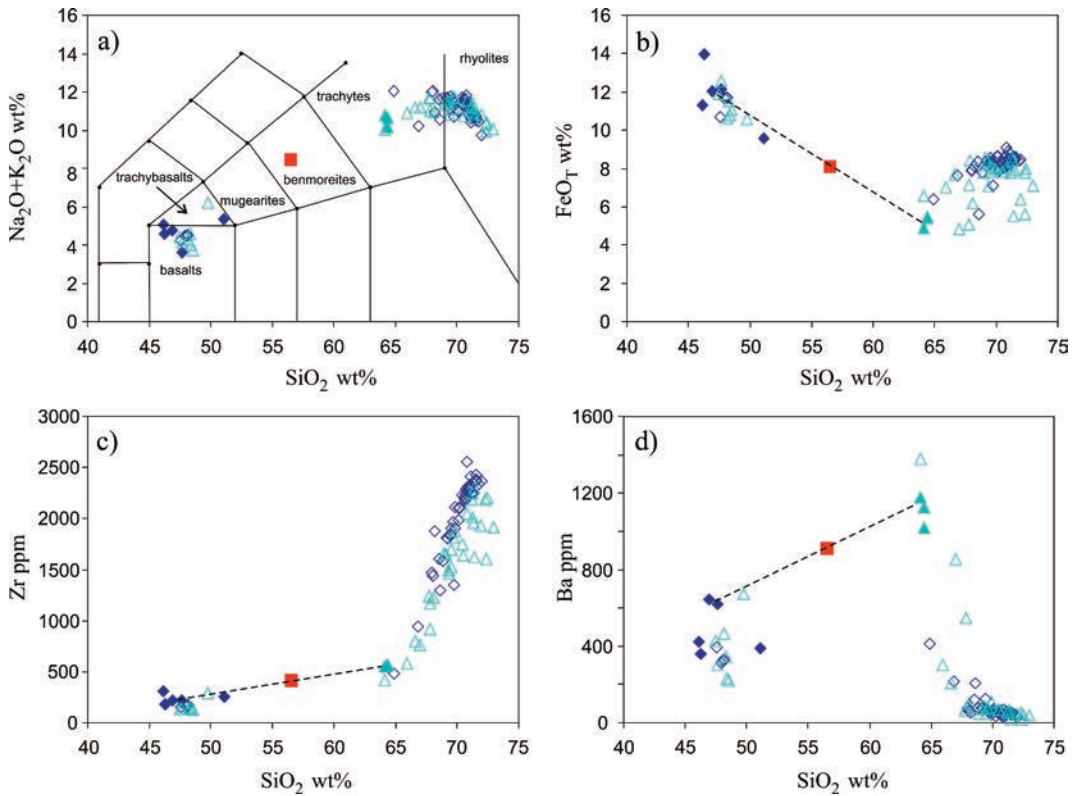


Figure 2. Comparison between bulk rock compositions of the benmoreitic lava and mafic and felsic rocks from Pantelleria. a): TAS classification diagram; b): SiO₂ vs FeO_T; c), d): SiO₂ vs selected trace elements. Square: benmoreitic lava; diamonds: data from Civetta et al., 1998 (the filled diamonds represent mafic rocks older than 50 ka); triangles: data from White et al., 2009 (the filled triangles represent metaluminous trachytes). Dotted line: mixing lines joining basalts older than 50 ka and metaluminous trachytes (see discussion for explanation).

(Cr₂O₃ ~ 25 wt.%) are peculiar to the Fo₈₄₋₈₆ cores, whereas rims include magnetite grains. Olivines with reverse zoning from Fo₄₄₋₅₃ to Fo₅₈₋₅₉ and rounded shape or skeletal rims crowded with magnetite inclusions are sporadic (Figure 5b, c). Olivine microphenocrysts and microlites show hopper to skeletal textures and a nearly homogeneous composition Fo₅₈₋₆₀ (Figure 5d) suggesting a moderate degree of undercooling.

The abundant microphenocrysts and grains of Ti-magnetite (usp = 65-72 mol %) occur together with minor ilmenite (ilm = 94-96 mol %), which is mostly found as microlites in the groundmass.

Trace elements in clinopyroxene

In order to investigate the origin of clinopyroxene, trace element contents were determined in the three types of pyroxene found in the sample: (i) euhedral phenocrysts with relatively homogeneous diopsidic composition (diopside phenocrysts in Figure 6); (ii) augitic pyroxene, both rounded phenocrysts and resorbed cores (augite phenocrysts in Figure 6), and (iii) pinkish diopside mantling augitic resorbed cores (Figure 6, Table 1). The pinkish microphenocrysts in the groundmass were not analyzed due to their small size and skeletal

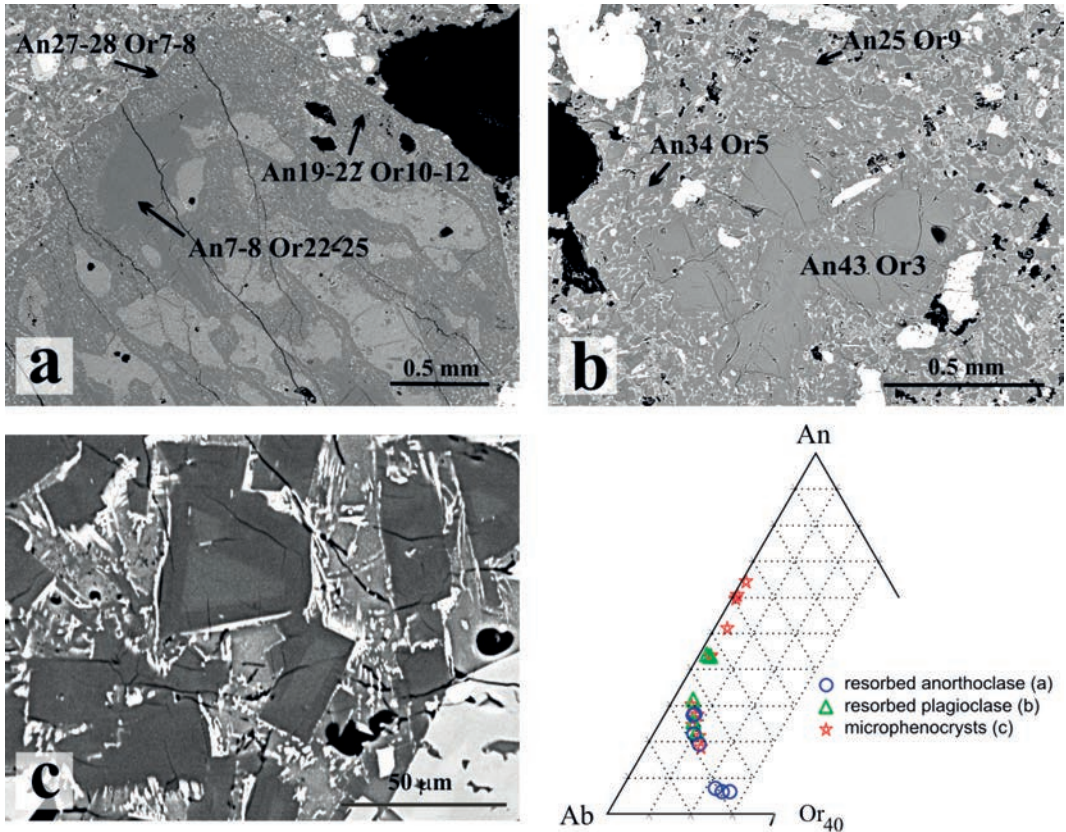


Figure 3. Back-scattered electron images representative of the different types of feldspars. a) spongy cellular textures in resorbed anorthoclase. Large cells filled by groundmass material (light grey) occupy the core of the crystal; b) crystals with resorbed cores of andesine plagioclase surrounded by a mantle of oligoclase showing finely spongy-cellular textures; c) zoned microphenocrysts (Ca-rich cores) and microlites of plagioclase in the groundmass; d) feldspar composition plotted in the An-Ab-Or mol% ternary diagram.

texture. The clinopyroxene from the Cudde Rosse alkali-basaltic scoria cone were also analyzed for comparison.

Diopside phenocrysts have incompatible element and REE contents close to those of alkali basalt pyroxenes (Figure 6) and nearly parallel REE patterns. The La_N/Lu_N ratio ranges from 1.4 to 1.9 in the diopside phenocrysts and from 1 to 1.5 in pyroxene from the Cudde Rosse basalt, whereas the Gd_N/Lu_N ratio ranges from 3.3 to 3.7 and 2.5 to 3.3, respectively.

The augite phenocrysts (Figure 6) show nearly homogeneous composition, close to those of the Fe-rich pyroxenes in Pantelleria trachytes (White et al., 2009 and unpublished data). La_N/Lu_N ratios (1.3-1.7) overlap with those of diopside phenocrysts, whereas Gd_N/Lu_N ratios decrease down to 1.6-1.9. The augite phenocrysts are also characterized by: (i) generally higher REE contents due to the more evolved (trachytic) magma composition (i.e. richer in incompatible elements) with respect to alkali basalt pyroxene,

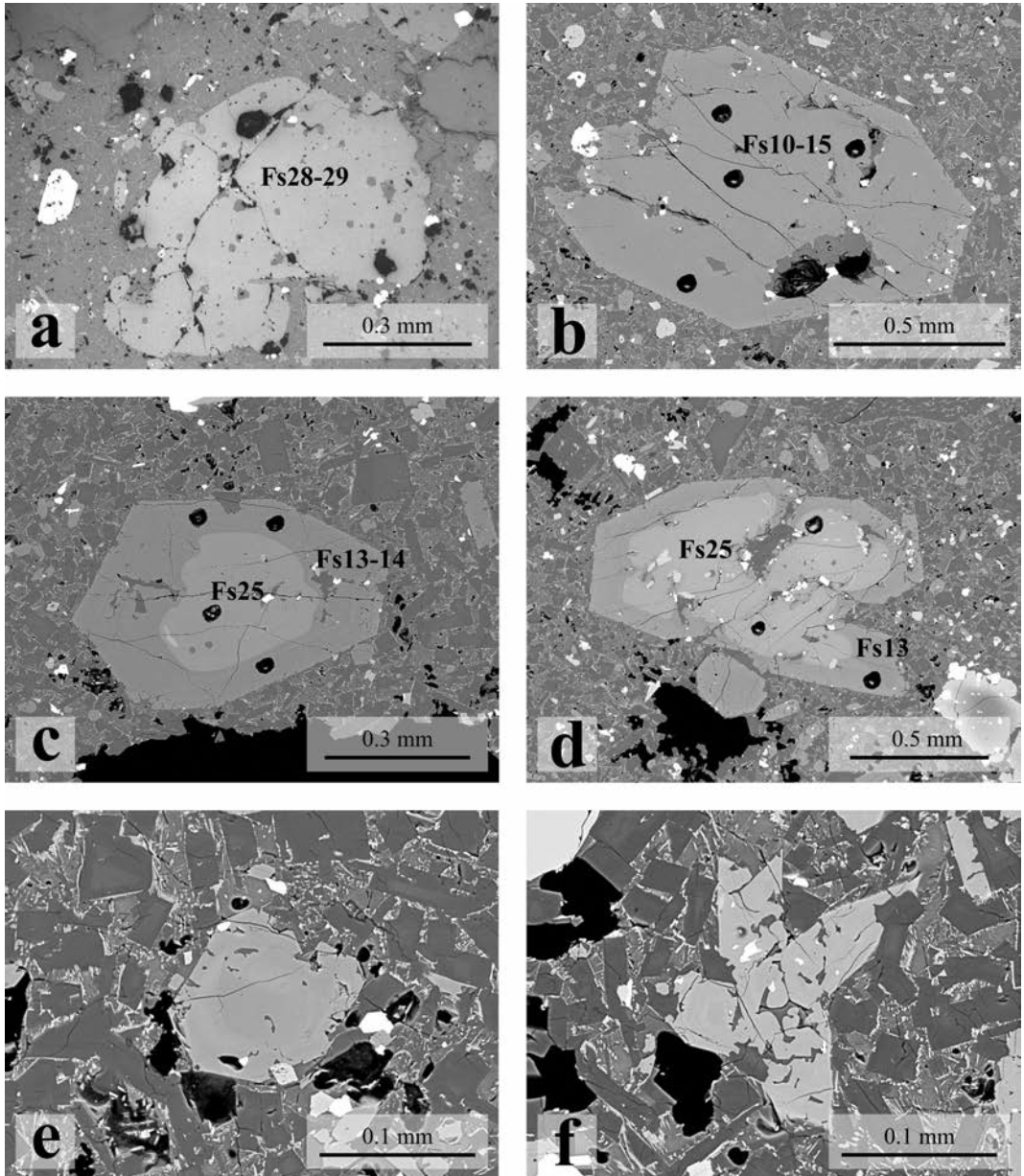


Figure 4. Representative images of different types of clinopyroxene. a) hedembergite phenocryst with rounded shape and embayment on the rim (reflected light); b) euhedral diopside phenocryst (BSE image). Spongy cellular textures and resorption channels near the rim (on the right) reveal incipient dissolution; c, d) BSE image of reverse-zoned crystals; e), f) microphenocrysts showing skeletal texture and sector zoning (BSE image). The black spots in b, c and d are holes generated by laser ablation.

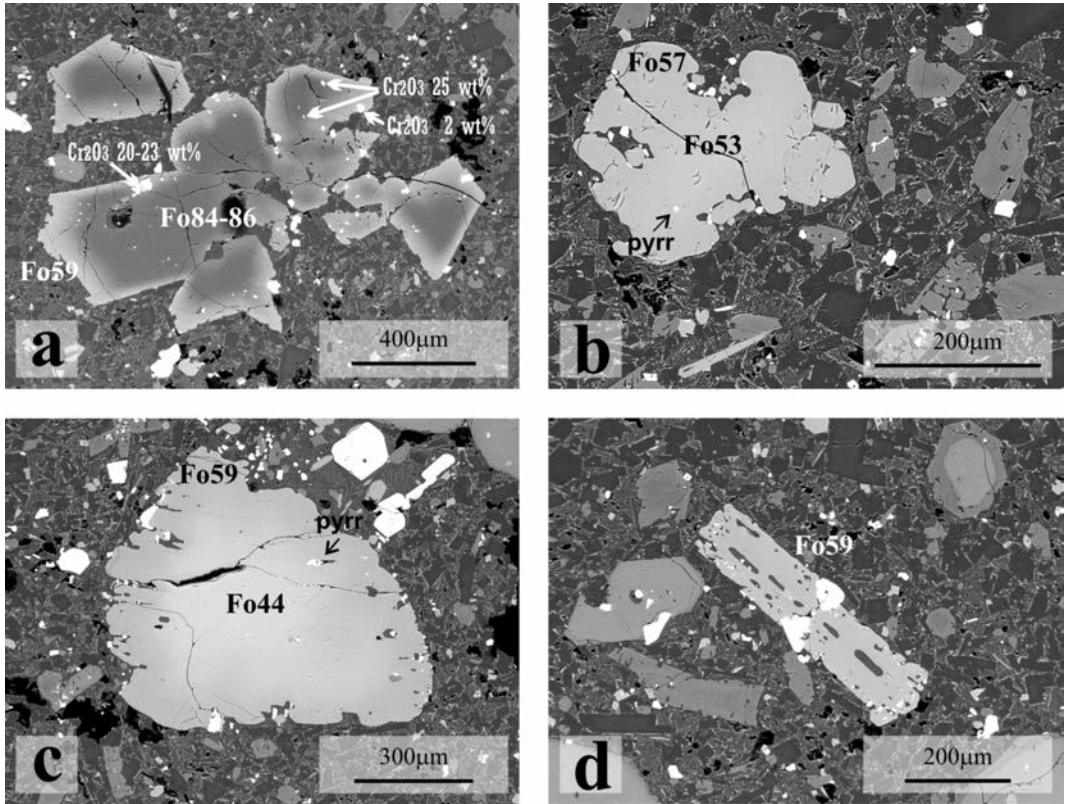


Figure 5. Back-scattered electron images of olivine. a) normal-zoned olivine with large Mg-rich cores hosting Cr-spinel inclusions (white spots) - note the high Cr_2O_3 wt.% content; b, c) anhedral, reverse-zoned olivine with pyrrhotite inclusion; d) tabular olivine microphenocryst showing hopper to skeletal texture due to intermediate/rapid growth rates determined by increasingly higher degrees of undercooling.

(ii) a negative Eu anomaly that reflects the Eu depletion of the (trachytic) melt due to abundant plagioclase fractionation from mafic parental melts.

At a comparable Mg#, the incompatible trace element and REE contents of the pinkish pyroxene are higher than those of diopside phenocrysts and generally intermediate between those of the trachytic and basaltic end members, except for the higher Ta, Zr, Hf contents (Figure 6) and La_N/Lu_N ratio (2.7-4). According to Coish and Taylor (1979), the high TiO_2 and Al_2O_3 contents of pinkish pyroxene may be due to the fast cooling

rate, as indicated by its skeletal texture in the groundmass. The rapid growth induced by fast cooling possibly affected not only the Ti and Al contents but also the partitioning of a few high field strength elements (Zr, Hf, Ta) and REE.

Discussion

The petrography and mineral chemistry of the benmoreite lava collected at the top of the Montagna Grande trachytic lava pile reveal distinct mineral parageneses and disequilibrium textures (resorptions, overgrowths, undercooling

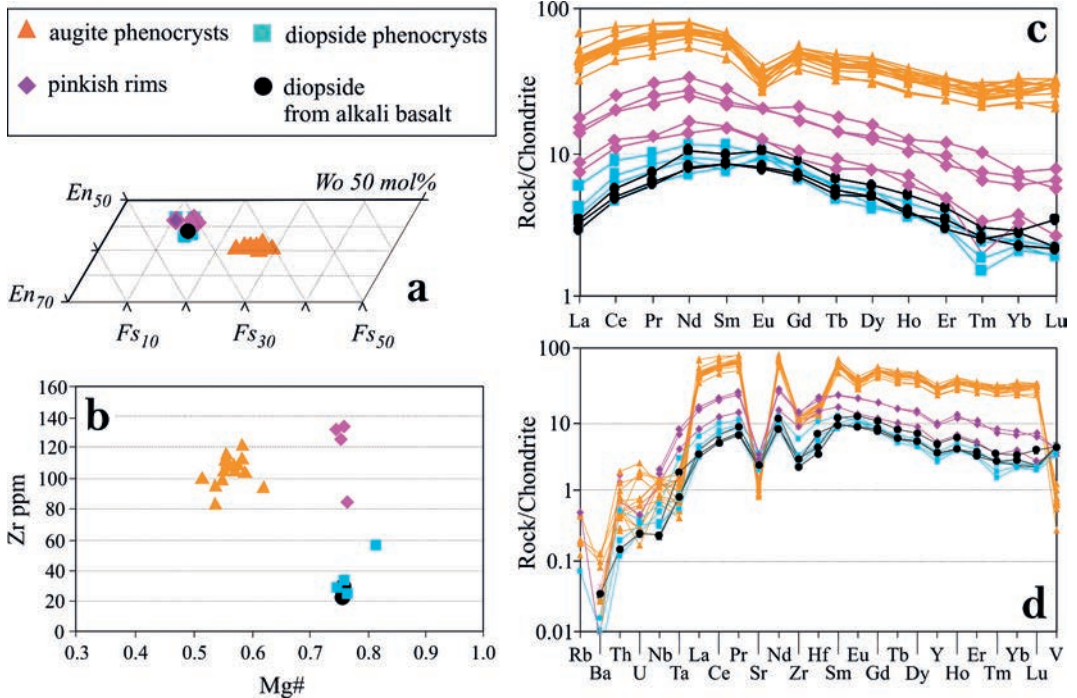


Figure 6. Trace element chemistry of diopsidic and augitic clinopyroxene from the “benmoreite” lava. a) clinopyroxene composition plotted in the Wo-En-Fs mol% ternary diagram; b) plot of Zr vs. Mg-number in clinopyroxenes; c) chondrite-normalized REE patterns and d) multi-element variation plot of trace elements in clinopyroxene (normalisation values from McDonough and Sun, 1995). Trace elements in clinopyroxenes from the Cuddie Rosse alkali-basaltic scoria cone are also reported for comparison. Note the occurrence of two main groups of pyroxene: i) diopside phenocrysts whose mineral chemistry is akin to that of the basaltic clinopyroxene are assumed to be representative of the basaltic end-member; ii) augitic phenocrysts inherited from a more evolved magma (the trachytic end member). Pinkish diopside has an intermediate trace element composition, except for the higher content in some HFS elements (Zr, Ta, Hf). See text for details.

textures) that may be ascribed to two distinct magma end-members from which the different mineral assemblages crystallized. The evolved end member comprises anorthoclase augite, and resorbed Na-Ca plagioclase (An_{32-43}), which are commonly found in the trachytic products of Pantelleria, and rare Fe-rich olivine (Fo_{44-53}). Mineral relicts of the mafic end member are represented by variably resorbed Fo_{84-86} olivine spotted with Cr-spinel inclusions. Trace elements in pyroxene also highlight the occurrence of

diopsidic phenocrysts related to basaltic magmas. Plagioclase phenocrysts inherited from a basaltic end-member are absent. Minerals with intermediate compositions (An_{64-25} plagioclase, Fo_{58-60} olivine, Fs_{10-14} clinopyroxene) occur as microphenocrysts and microlites or as rims around phenocrysts; they represent a mineral assemblage crystallized from a melt with intermediate composition between basalt and trachyte. These characteristics indicate that the Montagna Grande benmoreite is a hybrid rock

originating from mixing between trachytic and basaltic magmas.

Note that this is the first discovery of mafic magma within the caldera, even if only as an end-member of a hybrid rock.

Characteristic of the two end members

Mafic and felsic magmas erupted at Pantelleria, show differences in their petrographic characteristics, mineral composition and bulk rock chemistry, that are thought to be related either to a different genesis or, alternatively, to different petrogenetic processes during the magma evolution in shallow reservoirs (Civetta et al., 1998; Avanzinelli et al., 2004; White et al., 2009). The mineral chemistry and the bulk rock composition of the benmoreitic lava allow to make some inferences on the main characteristics of the mafic and felsic magmas involved in the mixing process.

Mafic end member. According to Civetta et al. (1998), two groups of basalts can be distinguished at Pantelleria: (i) a high $\text{TiO}_2\text{-P}_2\text{O}_5$ group older than 50 ka B.P. and a (ii) low $\text{TiO}_2\text{-P}_2\text{O}_5$ group younger than 50 ka (i.e. erupted after the Green Tuff). The older basalts have a nearly aphyric texture with phenocrysts of Fo-rich olivine (up to Fo_{85}) containing Cr-spinel inclusions ($\text{Cr}/\text{Cr}+\text{Al} = 0.40\text{-}0.42$) and diopsidic clinopyroxene. According to these authors, plagioclase occurs only as a groundmass phase. Basalts erupted after the Green Tuff eruption are instead porphyritic and seriate-textured with abundant Ca-rich plagioclase ($\text{An}_{60\text{-}80}$) and minor $\text{Fo}_{75\text{-}80}$ olivine and augite/diopside pyroxene (Civetta et al., 1998; Avanzinelli et al., 2004; Gioncada and Landi, 2010). The age of the most recent basalts (Cuddie Rosse scoriae cone in the NW part of the island) has been estimated to be around 20 ka (Mahood and Hildreth, 1986). These are almost contemporaneous to the eruption of the youngest trachytic lava flow within the caldera, dated at around 28 ± 16 ka (Mahood and Hildreth, 1986).

Mg-rich olivine (i.e. up to $\text{Fo}_{84\text{-}86}$) with Cr-spinel inclusions is the most abundant and significant mineral phase pertaining to the mafic end member of the hybrid benmoreite. Olivine with such a Mg-rich composition does not occur in the basalts younger than 50 ka. In particular, the composition of olivine in equilibrium in the Cuddie Rosse alkali basalts (around 20 ka) is $\sim \text{Fo}_{80}$ (Gioncada and Landi, 2010). The characteristics of the mafic end member in the hybrid benmoreite (abundance of olivine $\text{Fo}_{84\text{-}86}$ together with rare diopsidic phenocrysts and the absence of Ca-rich plagioclase phenocrysts) are all comparable with those of the high $\text{TiO}_2\text{-P}_2\text{O}_5$ alkali-basalts erupted before the Green Tuff eruption. Note that high $\text{TiO}_2\text{-P}_2\text{O}_5$ basalts also poured out during the historical submarine eruption of 1891 offshore the northwest coast of the island (Washington, 1909). White (2009) also reports the occurrence of a high $\text{TiO}_2\text{-P}_2\text{O}_5$ hawaiiite lava (Khattibucale hawaiiite) erupted after the Green Tuff eruption. We conclude that high $\text{TiO}_2\text{-P}_2\text{O}_5$ basalts also erupted in recent times: the age-related chemical subdivision into high/low -TiO_2 and $\text{-P}_2\text{O}_5$ basalts (Civetta et al., 1998) should therefore be reassessed.

Avanzinelli et al. (2004) suggest that basalts older than 50 ka crystallized at depths greater than 25 km (i.e. well below the inferred Moho at a depth of around 20 km, Civile et al., 2008), whereas post-caldera basalts likely ponded at shallower levels, as confirmed by volatile contents in melt inclusions in pyroxene and olivine from Cuddie Rosse products that yield entrapment pressures of around 2 kb (~ 7 km) (Gioncada and Landi, 2010). Based on these considerations, we can conclude that the Montagna Grande hybrid benmoreite rock originated by the intrusion of batches of a deep-seated, $\text{TiO}_2\text{-P}_2\text{O}_5$ -rich mafic magma into a shallow trachytic magma body.

Felsic end-member. Trachytes at Pantelleria show different degrees of evolution, from comenditic

trachytes to pantelleritic trachytes, which are reflected in their different mineral chemistry (White et al., 2009; Romengo, 2011). A comparison between the mineral compositions of the femic end member in the benmoreitic lava and those of trachytic rocks in literature (White et al., 2005; 2009; Romengo, 2011) suggest the involvement of a relatively poorly evolved trachytic magma characterized by abundant anorthoclase $Ab_{68-70}An_{6-8}Or_{23-26}$, clinopyroxene Fs_{25-28} and minor plagioclase An_{32-43} as resorbed cores. These compositions are close to those found in metaluminous trachytes by White et al. (2009) (clinopyroxene Fs_{26-32} , anorthoclase $An_{7-9}Or_{20-22}$ and resorbed cores of plagioclase An_{29-34}). Both resorbed anorthoclase and augite are abundant in the benmoreitic lava and show nearly homogeneous composition. Furthermore, the homogeneous trace element signature of the augitic clinopyroxenes ensures that they represent a single crystal population, associated with a single trachytic magma. Conversely, Fe-rich olivine (Fo_{44-53}), has compositions quite different from that of the phenocrysts in trachyte (usually olivine $Fo < 30$). Possibly, Fe-rich olivines are relicts of cognate crystals related to felsic melts less evolved than the trachytic magmas usually erupted at Pantelleria.

Based on chemical data from literature, to reproduce the bulk chemistry of benmoreite is required about 45 wt.% of basalt (a high TiO_2 - P_2O_5 basalt, Civetta et al., 1998) and 55 wt.% of trachyte (a metaluminous trachyte, White et al., 2009) (Figure 2). Conversely, if a basalts younger than 50 ka is used as mafic end member, the basalt/trachyte mixing model is not consistent with the content of several major and trace elements in the hybrid Benmoreite (e.g. alkali, Al_2O_3 , TiO_2 , Zr, La).

Insights into the origin of the trachyte magma and the Daly gap

The genesis of trachytes at Pantelleria has long been investigated using chemical, mineralogical

and isotopic approaches along with thermodynamic modelling. Traditional petrochemical investigations led to the development of two contrasting petrogenetic models, i.e. (i) crystal fractionation, which assumes consanguinity between basalts and trachytes, and (ii) remelting of mafic cumulates at the base of the crust. The crystal chemistry of pyroxenes, together with other petrological considerations, led Avanzinelli et al. (2004) to prefer the cumulate partial-melting model. Lowenstern and Mahood (1991) proposed the partial-melting model also on the basis of the low volatile content in pantellerite magmas. Recent experimental petrology and melt inclusion studies (Di Carlo et al., 2010; Gioncada and Landi, 2010; Romengo, 2011) question the assumption of low volatile contents in the felsic magmas of Pantelleria, since pantellerites were found to contain up to 4-4.5 wt.% H_2O . Protracted fractional crystallization starting from alkali basaltic parental magmas was proposed on the basis of major and trace element data, isotope chemistry and stratigraphic relationships between mafic and felsic volcanic rocks (Civetta et al., 1998; White et al., 2009). The fact that over the last 50 ka mafic magmas have erupted outside the caldera rim only (Mahood and Hildreth, 1986; Civetta et al., 1988; 1998) is thought to be due to the blocking role of the felsic low-density magma chamber. Although this study documents the arrival of a basaltic magma batch (although indirectly, as a ghost mafic end-member in a mixed rock) within the low-density trachyte magma chamber, it confirms that mafic magmas have difficulty in finding an ascent pathway in the central portion of the island. We have no robust estimates of the volume of magma (neither of trachyte reservoirs nor of the basalt magma batches). We can only assess that the volume of basaltic magma erupted within the caldera in the past 50 ka is negligible compared to that of the trachyte: about 3 km^3 of trachytes were erupted during the development

of the Montagna Grande-Monte Gibele lava pile (Mahood and Hildreth, 1986), whereas the erupted basalts represent ~ 45 wt.% of a single lava flow with a volume of only 10^4 m³.

The occurrence of basalt-trachyte mixing events cannot be considered definitive evidence of a parent-daughter relationships between basaltic and trachytic magmas (the crystal fractionation model). It simply demonstrates that mafic melts intruded the cooling felsic magma chamber, straying from their usual pathway (i.e. northwards, beyond the caldera rim). The supply of basaltic magma from the upper mantle and melting of gabbro-cumulates at the base of the crust are separate phenomena which may occur simultaneously and drive magma evolution. If the "re-melting" model is taken into account, the periodic intrusion of small batches of mafic magmas into the shallow reservoirs cannot drastically alter the bulk chemical composition of the melt-derived trachytes, given the high mass proportion of trachytic magma. In this context, the production of intermediate magmas must be regarded as an occasional and transient phenomenon strictly associated with mixing events at the base of the reservoir. The hybrid melts, mixed and homogenized with the host trachytes, are consequently lost. A trace of their existence may be preserved only when the hybrid magma is erupted before complete mixing occurs. Following this hypothesis, mixing between basaltic melts and trachytes derived by partial melting could affect the evolution of the magma, possibly determining minor differences in the degree of peralkalinity and in the trace element chemistry of the felsic magmas.

Conclusions

The benmoreite lava flow cropping out at the top of the Montagna Grande trachyte lava pile does not represent a melt derived from a basaltic parent but is the result of mixing between

basaltic and trachytic magmas. Our results thus confirm that intermediate magmas formed by crystal fractionation of basalts have not been erupted at Pantelleria. Although the benmoreite lava erupted inside the Cinque Denti caldera in recent times (44-28+/-16 ka), the basaltic end-member shows the same mineral chemistry as the TiO₂-P₂O₅-rich basalts erupted before the collapse of the caldera (age > 50 ka). The primitive TiO₂-P₂O₅ rich magmas which likely originated in the mantle at depths \geq 18 km were thus also produced in recent times. Lastly, this study demonstrates that small batches of basaltic melts were able to intrude the shallow, and low-density, felsic magma body and mix with the resident magma. Whatever the origin of the trachytes (consanguinity between basalts and trachytes or re-melting of mafic cumulates), intrusion of basalts into shallow felsic reservoirs have to some extent affected the magma evolution at Pantelleria.

Acknowledgments

Patrizia and Silvio dedicate this paper to the memory of Nancy (Nunzia) Romengo who enthusiastically studied several aspects of Pantelleria geology during her graduation and PhD Theses.

We wish to thank two anonymous Reviewers for their helpful and constructive comments.

This work has been partly supported by the INGV-DPC project: "Monitoring and research activity at Stromboli and Panarea".

References

- Avanzinelli R., Bindi L., Menchetti S. and Conticelli S. (2004) - Crystallization and genesis of peralkaline magmas from Pantelleria Volcano, Italy: an integrated petrological and crystal-chemistry study. *Lithos*, 73, 41-69.
- Calanchi N., Colantoni P., Rossi P.L., Saitta M. and Serri G. (1989) - The Strait of Sicily continental rift systems: physiography and petrochemistry of the submarine volcanic centres. *Marine Geology*, 57, 55-83.

- Catalano S., De Guidi G., Romagnoli G., Torrisi S. and Tortorici L. (2008) - The migration of plate boundaries in the SE Sicily: influence of the large-scale kinematic model of African promontory in southern Italy. *Tectonophysics*, 449, 41-63.
- Coish R.A. and Taylor L.A. (1979) - The effects of cooling rate on texture and pyroxene chemistry in DSDP Leg 34 basalt: a microprobe study. *Earth and Planetary Science Letters*, 42, 389-398.
- Civetta L., Cornette Y., Crisci G., Gillot P.Y., Orsi G. and Requejo C.S. (1984) - Geology, geochronology and chemical evolution of the island of Pantelleria. *Geological Magazine*, 121, 541-562.
- Civetta L., Cornette Y., Gillot P.Y. and Orsi G. (1988) - The eruptive history of Pantelleria (Sicily Channel) in the last 50 ka. *Bulletin of Volcanology*, 50, 47-57.
- Civetta L., D'Antonio M., Orsi G., Tilton G.R. (1998) - The geochemistry of volcanic rocks from Pantelleria island, Sicily channel: petrogenesis and characteristics of the mantle source region. *Journal of Petrology*, 39: 1453-1491.
- Civile D., Lodolo E., Tortorici L., Lanzafame G. and Brancolini G. (2008) - Relationships between magmatism and tectonics in a continental rift: The Pantelleria Island region (Sicily Channel, Italy). *Marine Geology*, 251, 32-46.
- Di Carlo I., Rotolo S.G., Scaillet B., Buccheri V. and Pichavant M. (2010) - Phase equilibrium constraints on pre-eruptive conditions of recent felsic explosive volcanism at Pantelleria Island, Italy. *Journal of Petrology*, 51, 2245-2276.
- Ferla P. and Meli C. (2006) - Evidence of magma mixing in the "Daly Gap" of alkali suites: a case study from the enclaves of Pantelleria (Italy). *Journal of Petrology*, 47, 1467-1507.
- Finetti I. (1984) - Geophysical study of the Sicily Channel rift zone. *Bollettino di Geofisica Teorica e Applicata*, 23, 3-28.
- Gioncada A. and Landi P. (2010) - The pre-eruptive volatile contents of recent basaltic and pantelleritic magmas at Pantelleria (Italy). *Journal of Volcanology and Geothermal Research*, 189, 191-201.
- Lowestern J.B. and Mahood G.A. (1991) - New data on magmatic H₂O contents with implications for petrogenesis and eruptive dynamics at Pantelleria. *Bulletin of Volcanology*, 54, 78-83.
- Mahood G.A. and Hildreth W. (1986) - Geology of the peralkaline volcano at Pantelleria, Strait of Sicily. *Bulletin of Volcanology*, 48, 143-172.
- McDonough W.F. and Sun S.S. (1995) - The composition of the Earth. *Chemical Geology*, 120, 223-253.
- Mungall J.E. and Martin R.F. (1995) - Petrogenesis of basalt-comendite and basalt-pantellerite series, Terceira Azores, and some implications for the origin of ocean-island rhyolites. *Contributions to Mineralogy and Petrology*, 119, 43-55.
- Mushkin A., Stein M., Halicz L. and Navon O. (2002) - The Daly gap: low-pressure fractionation and heat loss from a cooling magma chamber. *Geochimica et Cosmochimica Acta*, 66, Supplement 1, A539.
- Orsi G., Ruvo L. and Scarpati C. (1991) - The recent explosive volcanism at Pantelleria. *Geologische Rundschau*, 80, 187-200.
- Peccerillo A., Barberio M.R., Yirgu G., Ayalew D., Barbieri M. and Wu T.W. (2003) - Relationships between mafic and peralkaline silicic magmatism in continental rift settings: a petrological, geochemical, and isotopic study of the Gedemsa volcano, central Ethiopian rift. *Journal of Petrology*, 44, 2003-2032.
- Romengo N. (2011) - Relationships between mafic and felsic magmatism at Pantelleria: a petrological study on intermediate trachyte magmas. PhD Thesis, University of Palermo.
- Rotolo S.G., Castorina F., Cellura D. and Pompilio M. (2006) - Petrology and Geochemistry of submarine volcanism in the Sicily Channel Rift. *Journal of Geology*, 114/3, 355-365.
- Rotolo S.G., La Felice S., Mangalaviti A. and Landi P. (2007) - Geology and petrochemistry of the recent (< 25 ka) silicic volcanism at Pantelleria Island. *Bollettino della Società Geologica Italiana*, 126, 191-208.
- Scaillet B. and Macdonald R. (2001) - Phase relations of peralkaline silicic magmas and petrogenetic implications. *Journal of Petrology*, 42, 825-845.
- Scaillet B. and Macdonald R. (2003) - Experimental constraints on the relationships between peralkaline rhyolites of the Kenya Rift Valley. *Journal of Petrology*, 94, 1867-1894.
- Scaillet B. and Macdonald R. (2006) - Experimental and thermodynamic constraints on the sulphur yield of peralkaline and Metaluminous silicic flood eruptions, *Journal of Petrology*, 47, 1413-1437.
- Scaillet S., Rotolo S.G., La Felice S. and Vita G. (2011) - High resolution ⁴⁰Ar/³⁹Ar chronostratigraphy of the

- post-caldera (< 20 ka) volcanic activity at Pantelleria, Sicily Strait. *Earth and Planetary Science Letters*, 309, 280-290. doi:10.1016/j.epsl.2011.07.009
- Streck M.J. (2008) - Mineral textures and zoning as evidence for open system processes. In: *Reviews in Mineralogy & Geochemistry: Minerals, inclusions and volcanic processes*. (eds): Keith D. Putirka and Frank J. Tepley III. 69, 595-622.
- Speranza F., Landi P., D'Ajello Caracciolo F. and Pignatelli A. (2010) - Paleomagnetic dating of the most recent silicic eruptive activity at Pantelleria (Strait of Sicily). *Bulletin of Volcanology*, 72, 847-858.
- Speranza F., Di Chiara A. and Rotolo S.G. (2011) - Correlation of welded ignimbrites on Pantelleria, using paleomagnetism. *Bulletin of Volcanology*, 74/2, 341- 357. doi:10.1007/s00445-011-0521-9
- Tiepolo M., Bottazzi P., Palenzona M. and Vannucci R. (2003) - A laser probe coupled with ICP-double-focusing sector-field mass spectrometer for in situ analysis of geological samples and U-Pb dating of zircon. *Canadian Mineralogist*, 41, 259-272.
- Villari L. (1974) - The Island of Pantelleria. *Bulletin of Volcanology*, 38, 680-724.
- White J.C., Parker D.F. and Ren M. (2009) - The origin of trachyte and pantellerite from Pantelleria, Italy: insights from major elements, trace elements, and thermodynamic modelling. *Journal of Volcanology and Geothermal Research*, 179, 33-55. doi:10.1016/j.volgeores.2008.10.007.
- White J.C., Ren M. and Parker D.F. (2005) - Variation in mineralogy, temperature, and oxygen fugacity in a suite of strongly peralkaline lavas and tuffs, Pantelleria, Italy. *Canadian Mineralogist*, 43, 1331-1347.
- Washington H.S. (1909) - The submarine eruptions of 1831 and 1891 near Pantelleria. *American Journal of Science*, 237, 131-150.

Submitted, December 2011 - Accepted, April 2012